OPTICAL PROPERTIES OF GOLD NANOPARTICLES PRODUCED BY THE ASSEMBLY OF SIZE-SELECTED CLUSTERS: COVERING THE FULL VISIBLE WAVELENGTH RANGE IN THE SMALLEST PARTICLE SIZE REGIME

Stefan VAJDA[a1,b,*], Gary P. WIEDERRECHT[a2,b], Alexandre BOUHELIER[a3,b,+], George Y. TIKHONOV[a4,++], Nancy TOMCZYK[a5], Byeongdu LEE[c1], Sönke SEIFERT[c2] and Randall E. WINANS[c3]

[a] *Chemistry Division, Argonne National Laboratory, Argonne, IL 60439, U.S.A.;*
 e-mail: [1] *vajda@anl.gov,* [2] *wiederrecht@anl.gov,* [3] *alexandre.bouhelier@u-bourgogne.fr,*
 [4] *tikhonov@email.arizona.edu,* [5] *tomczyk@anl.gov*
[b] *Center for Nanoscale Materials, Argonne National Laboratory, Argonne, IL 60439, U.S.A.*
[c] *X-ray Science Division, Argonne National Laboratory, Argonne, IL 60439, U.S.A.;*
 e-mail: [1] *blee@anl.gov,* [2] *seifert@anl.gov,* [3] *rewinans@anl.gov*

Dedicated to the memory of Professor Jaroslav Koutecký.

The tunability of the optical properties of small gold nanoparticles assembled from size-selected Au_{6-10} clusters on the surface of indium-tin-oxide glass support was studied as a function of gold particle size and shape using UV-VIS and dark-field microscopy techniques. The size and shape of gold nanoparticles was determined by employing synchrotron X-ray scattering. The obtained spectra show that a 350 nm wavelength range is accessible by proper tuning the size and shape of the studied nanoparticles with 1–2.5 nm main size and asymmetric vs symmetric form.
Keywords: Gold nanoparticles; Gold clusters; Dark-field microscopy; GISAXS; Synchrotron X-ray scattering; UV-VIS spectroscopy; Size-selected cluster deposition.

Interaction of light with metal nanoparticles produces a range of physical and chemical phenomena that impact an extraordinary breadth of basic science research and technological applications. Areas of interest include surface-enhanced Raman scattering (SERS)[1,2], photocatalysis[3], surface plas-

mons[4], molecular sensors[5], and electronic coherences for nanophotonics applications[6], to name only a few. Also, due to energy transfer in organized arrays of closely spaced metal nanoparticles, there is interest in these new materials for light harvesting applications[7,8]. The recent interest in metal-nanoparticle-based structures is particularly driven by advances in chemical synthesis and lithographic techniques that reliably produce complex shapes, narrow size distributions, and hybrid core-shell materials. These efforts make clear that the optical properties of metal nanoparticles can be tailored to facilitate a desired photochemical or photophysical response. The tunability of the UV-VIS properties in the smallest achievable particle size-regime is not yet a sufficiently explored field. Many studies suggest that noble metal clusters of only a few atoms show plasmon absorption bands, the source of many nanophotonic applications of metal nanoparticles. The very few in literature available papers on small cluster properties dealt with gas-phase clusters[9] or ligand-stabilized ones[10]. However, it is not established how the optical properties evolves with clusters and smallest nanoparticles as a function of size and, very importantly, shape. In the presented study, this central issue will be addressed by studying the UV-VIS properties of nanoparticles assembled from size-selected clusters as building blocks.

EXPERIMENTAL

Synthesis of Small Gold Nanoparticles from Deposited Size-Selected Clusters

The continuous beam of gold clusters was generated in a high-flux laser ablation cluster source which utilizes the frequency-doubled (532 nm) output of a Quantronix Nd YAG laser operating at 4.5 kHz (Fig. 1). During the ablation process, neutral as well as positively and negatively charged atoms and their aggregates are formed in the helium carrier gas. After leaving the 1-mm diameter nozzle of the cluster source, the beam of neutral and charged clusters is guided through a biased skimmer into the ion guide of the second differentially pumped vacuum stage and then into the third differentially pumped vacuum stage. The positively charged clusters are led and focused into the quadrupole mass spectrometer (Extrel) for mass analysis. Narrow cluster distributions in the size range Au_n^+, $n = 1, ... 10$, with one to four dominant sizes can be produced by optimizing the temperature of the clusters source, pressure of the helium carrier gas in the cluster source and potential settings on the individual ion optics elements of the beam line. After the desired cationic cluster distribution is produced, the indium-tin-oxide (ITO) covered glass substrate is translated into the cluster beam path. The kinetic energy of clusters landing on the surface is controlled by biasing the substrate to a desired voltage. Typical deposition energies are less than 0.5 eV/atom with the goal to avoid cluster fragmentation upon impact. The flux of clusters landing on the ITO support is monitored in real-time using a picoammeter (Keithley), which allows for precise determination of the surface coverage with clusters. Typical average deposition currents are in the order of tens to several hundreds of picoamperes, depending on

the size of clusters. All samples were prepared using the identical scheme: cluster size distributions consisting of Au_{6-10} and varying the surface coverage between 1 and 10% of atomic monolayer equivalent with the goal to form small gold nanoparticles. The chosen range of surface coverage was based on our former experiments showing considerable aggregation of gold clusters into nanometer-sized particles on various surfaces when exceeding surface coverages of about 5% of monolayer (ML)[11].

Determination of the Size of Gold Nanoparticles

Grazing-incidence X-ray scattering and the advanced photon source (GISAXS) of the Argonne National Laboratory was used to determine the size of gold nanoparticles and the thickness of the ITO layer. The GISAXS experiments were performed in a vacuum chamber equipped with a sample holder mounted on a goniometer. The sample holder is made of a brass rod with a milled flat surface on its end. X-rays produced in an undulator (12.0 keV) pass through a double-crystal monochromator ($\Delta E/E \sim 10^{-4}$) and a focusing mirror. The beam was scattered off the surface of the sample at and near the critical angle of the ITO-glass substrate. The scattered X-rays are detected by a nine-element mosaic CCD detector (150 × 150 mm) with a maximum resolution of 3000 × 3000 pixels[12]. The two-dimensional data are analyzed by taking cuts in the q_{xy} direction for horizontal information and in the q_z direction for vertical information (Fig. 2). From these data the distribution of particle width and height are calculated. Silver behenate is used to calibrate both horizontal and vertical q values for the given camera length prior to the experiment.
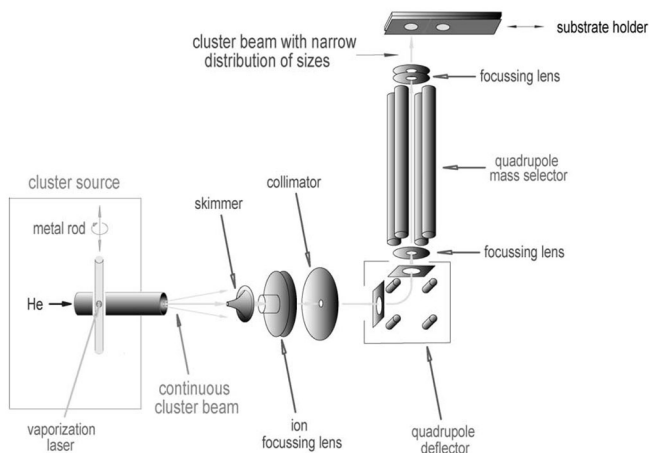

FIG. 1
Scheme of the experimental setup for size-selected cluster deposition

UV-VIS and Dark-Field Microscopy Characterization

Steady-state averaged absorption spectra were recorded using a Shimadzu UV-VIS spectrometer by exposing an approximately 5-mm^2 sample area to the incident light. In order to study the response from a small surface area, dark-field microscopy was employed. Dark-field spectroscopy provides a unique insight into the spectral properties of resonant particles by maximizing scattering from individual structures while keeping a low (dark) background from the substrate itself. Dark-field spectroscopy offers also the advantage of sensitivity in comparison to other spectroscopic techniques such as transmission or absorption spectroscopy at a single particle level. The absorption cross-section scales with the volume v of a particle whereas typical scattering cross-sections show a v^3 dependence. A standard inverted microscope (Olympus IX 71) retrofitted with a dark-field condenser to illuminate the substrate was used[13]. The condenser utilizes an annular stop to block the light emerging from the lens below angles that correspond to a numerical aperture (NA) of 0.8. To ensure proper dark-field illumination, the collection objective must have a lower NA than the dark-field condenser ensuring that only the light scattered by the object is collected. The scattered signal is then sent to a spectrograph and dispersed on a cooled CCD camera. The width of the slit and the resolving power of the collection objective define the lateral and spectral resolution. Individual scatterers were selected randomly and positioned on the optical axis by means of a piezoelectric flexure stage. The acquisition time of the spectra were comprised between 30 and 300 s depending on the amount of scattered intensity. Each spectrum was background-corrected by displacing the scattering center off the optical axis (typically 10 μm). The width of the slit was kept at 40 μm providing thus a reasonable amount of signal while maintaining a satisfactory spectral resolution. The scattered signals were dispersed by a 300 gr/mm ruled grating blazing at 500 nm. Under given conditions, a sample area with approximately 1-μm diameter was targeted. Taking into consideration the spatial resolution of the microscope, size of gold nanoparticles and the amount of gold material used, a single gold particle or only a very limited number of particles were expected to be found in the imaged area.
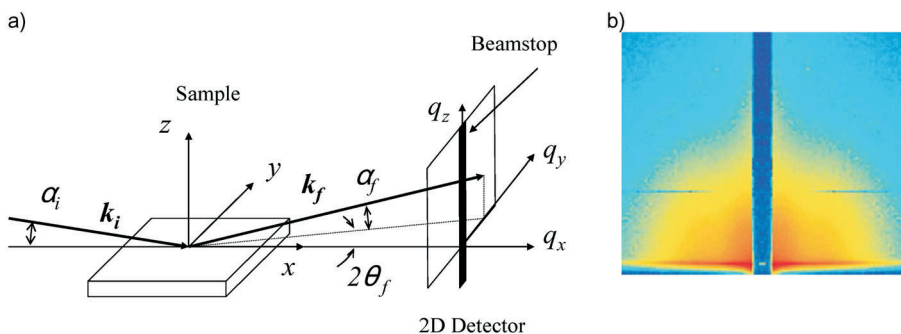

FIG. 2

a Schematic of GISAXS experiment. Incident X-ray beam (k_i) angle and scattered beam (k_f) are α_i and α_f, respectively. Scattering vectors q are calculated from $(4\pi/\lambda)\sin\theta_f$ where θ_f is the scattering half-angle and λ is the wavelength of the X-rays. b Typical two-dimensional GISAXS image

RESULTS

No detectable UV-VIS absorption was observed in the case of the sample with the lowest cluster coverage (1% ML). However, in the case of the samples with 6, 9 and 10% monolayer surface coverage, a distinct and very broad absorption band centered at around 520 nm emerged in the spectra. The position of the absorption peak did not exhibit a significant shift with increasing surface coverage, thus indicating that the average size of the light-absorbing particles does not change considerably when increasing the surface coverage up to 10% ML – an assumption supported by both available literature data and a control experiment performed in our lab. As reported in the literature for gold nanoparticles with diameters of several to tens of nanometers in diameter[14–19], their absorption peak shifts towards longer wavelengths with increasing particle size. In a control experiment, gold clusters were deposited without size selection on glass surfaces at vari-
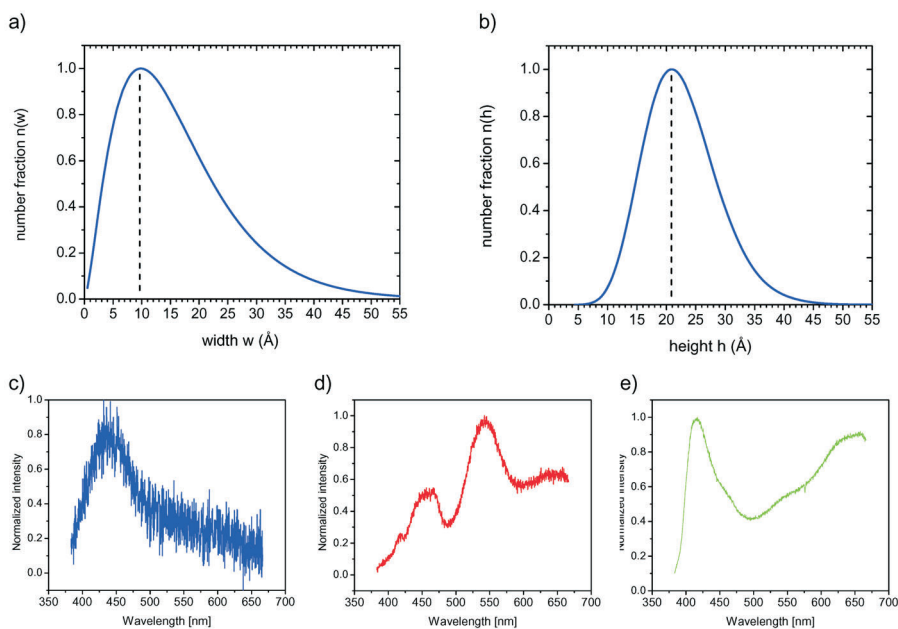

FIG. 3
Peak-normalized width (a) and height (b) distribution of gold nanoparticles assembled from Au_{6-10} clusters at 6% ML coverage on the ITO substrate. Peak-normalized dark-field microscopy spectra collected at various locations of the surface (c–e)

able coverages leading to the formation of up to several nanometers large nanoparticles – the obtained UV-VIS spectra showed a progressive shift of the absorption band from approximately 530–590 nm with growing particle size[20]. The structureless broad absorption peaks emerging in the spectra of the samples discussed in this paper were indicative of an ensemble of highly inhomogeneous particles.

6% Monolayer Gold Sample

The width and height distribution of the gold nanoparticles determined by GISAXS is plotted in Fig. 3a and 3b, respectively. The width of the particles is centered around 10 Å, their height around 21 Å, thus indicating highly asymmetrical tall structures. The dark-field microscopy responses of recorder at various locations on the gold-particle-covered surface area show
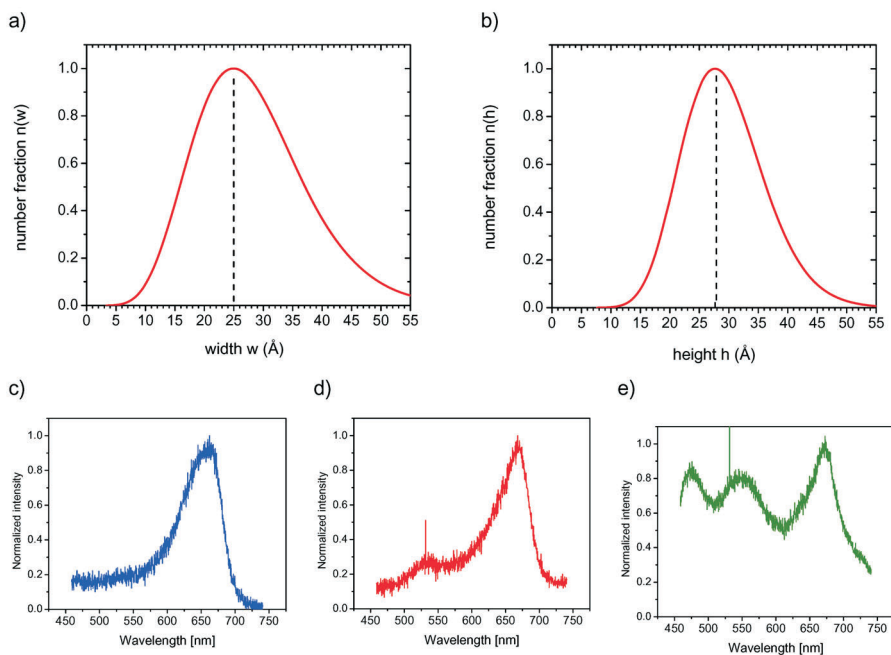

FIG. 4

Peak-normalized width (a) and height (b) distribution of gold nanoparticles assembled from Au_{6-10} clusters at 9–10% ML coverage on the ITO substrate. Peak-normalized dark-field microscopy spectra collected at various locations of the surface (c–e)

red-shifted absorption bands extending into the near infrared range (from 410 nm to approximately 700 nm, Fig. 3c–3e).

10% Monolayer Gold Sample

The width and height distribution of the gold nanoparticles determined by GISAXS is plotted in Fig. 4a and 4b, respectively. The width of the particles is centered around 25 Å, their height around 27 Å, thus indicating more spherical structures in contrast to the 6% ML sample. The dark-field microscopy responses recorded at various locations on the gold-particle-covered surface area show red-shifted absorption bands extending to around 750 nm (Fig. 4c–4e).

DISCUSSION AND CONCLUSIONS

The studied UV-VIS properties of small gold nanoparticles of various shapes indicate a very strong dependence of the UV-VIS properties of supported individual gold nanoparticles on their shape in the smallest-size regime. Moreover, these particles exhibited extraordinary stability; their optical properties as monitored by UV-VIS spectroscopy did not change by immersion of the samples into thiol-containing water solutions and after exposure to ozone used to burn off the thiols[21]. These studies are in their initial stage. However, the obtained results indicate the feasibility of controlled synthesis of highly stable size-selected gold clusters[11], and nanoparticles of desired size and shape[22,23] built of clusters. This allows for fine-tuning their optical properties. An additional tuning knob for the optical properties is the composition of the solvent. These control parameters, in addition to the highly size-specific chemical reactivity of gold clusters and small nanoparticles, are to be used for highly selective single molecule sensors, hierarchical nanophotonics structures as well as for nanophotocatalysis.

REFERENCES

1. Nie S. M., Emery S. R.: *Science* **1997**, *275*, 1102.
2. Kneipp K., Wang Y., Kneipp H., Perelman L. T., Itzkan I., Dasari R., Feld M. S.: *Phys. Rev. Lett.* **1997**, *78*, 1667 .
3. Subramanian V., Wolf E. E., Kamat P. V.: *J. Am Chem. Soc.* **2004**, *126*, 4943.
4. El-Sayed M. A.: *Int. Rev. Phys. Chem.* **2000**, *19*, 409.
5. Jackson J. B., Westcott S. L., Hirsch L. R., West J. L., Halas N. J.: *Appl. Phys. Lett.* **2003**, *82*, 257.
6. Wiederrecht G. P., Wurtz G. A., Hranisavljevic J.: *Nano Lett.* **2004**, *4*, 2121.
7. Atwater H.: *SPIE's **oe**magazine*, July 2002, pp. 42–44; http://oemagazine.com/fromtheMagazine/jul02/pdf/guidinglight.pdf
8. Hasobe T., Imahori H., Kamat P. V., Ahn T. K., Kim S. K., Kim D., Fujimoto A., Hirakawa T., Fukuzumi S.: *J. Am. Chem. Soc.* **2005**, *127*, 1216.
9. Collings B. A., Athanassenas K., Lacombe D., Rayner D. M., Hackett P. A.: *J. Chem. Phys.* **1994**, *101*, 3506.
10. Zheng J., Zhang C., Dickson R. M.: *Phys. Rev. Lett.* **2004**, *93*, 077402.
11. Vajda S., Winans R. E., Elam J. W., Lee B., Pellin M. J., Seifert S., Tikhonov G. Y., Tomczyk N. A.: *Top. Catal. (Special Issue)* **2006**, *39*, 161.
12. Seifert S., Winans R. E., Tiede D. M., Thiyagarajan P.: *J. Appl. Crystallogr.* **2000**, *33*, 782.
13. Bouhelier A., Bachelot R., Im J. S., Wiederrecht G. P., Lerondel G., Kostcheev S., Royer P.: *J. Phys. Chem. B* **2005**, 109, 3195.
14. Antoine R., Pellarin M., Palpant B., Broyer M., Prével B., Galletto P., Brevet P. F., Girault H. H.: *J. Appl. Phys.* **1998**, *84*, 4532.
15. Murillo L., Viera O., Vicuña E., Briano J., Castro M., Ishikawa Y., Irizarry R., Solá L.: "Growth Kinetics of Gold Nanoparticles", presented at Computational Nanoscience and Nanotechnology, www.cr.org **2002**.
16. Felidj N., Aubard J., Levi G., Krenn J. R., Hohenau A., Schider G., Leitner A., Aussenegg F. R.: *Appl. Phys. Lett.* **2003**, *82*, 3095.
17. Link S., Burda C., Wang Z. L., El-Sayed M. A.: *J. Chem. Phys.* **1999**, *111*, 1255
18. Okamoto T., Yamaguchi I.: *J. Phys. Chem. B* **2003**, *107*, 10321.
19. Sönnichsen C., Franzl T., Wilk T., von Plessen G., Feldmann J.: *New J. Phys.* **2002**, *4*, 93.
20. Vajda S., Tikhonov G. Y., Wiederrecht G.: Unpublished results.
21. Elam J. W., Pellin M. J., Tikhonov G. Y., Vajda S.: Unpublished results.
22. Vajda S., Winans R. E., Elam J. W., Lee B., Pellin M. J., Riley S. J., Seifert S., Tikhonov G. Y., Tomczyk N. A.: *Am. Chem. Soc., Div. Fuel Chem.* **2005**, *50*, 190.
23. Lee B., Seifert S., Riley S. J., Tikhonov G. Y., Tomczyk N., Vajda S., Winans R. E.: *J. Chem. Phys.* **2005**, *123*, 074701.